

Quantification of the carrier absorption losses in Si-nanocrystal rich rib waveguides at 1.54 μm

D. Navarro-Urrios,^{1,a)} A. Pitanti,¹ N. Daldosso,¹ F. Gourbilleau,² R. Rizk,² G. Pucker,³ and L. Pavesi¹

¹Laboratorio di Nanoscienze, Dipartimento di Fisica, Università di Trento, Via Sommarive 14, I-38050 Povo (Trento), Italy

²CIMAP, UMR CNRS 6252, 6 Boulevard Maréchal Juin, 14050 CAEN, France

³Fondazione Bruno Kessler, MicroTechnology Laboratory, Via Sommarive 18, 38050 Povo-Trento, Italy

(Received 5 December 2007; accepted 15 January 2008; published online 4 February 2008)

A detailed study of the carrier absorption (CA) mechanism in multilayered silicon-nanocrystals (Si-nc) rib waveguides is reported. A pump (532 nm) and probe (1535 nm) technique is used to assess two loss mechanisms due to optical excitation of the system: one characterized by slow (seconds) dynamics related to heating and the other characterized by fast (microsecond) dynamics associated to CA mechanisms within the Si-nc. CA losses increase with pumping flux of up to 6 dB/cm for 3×10^{20} photons/cm² s. By comparing the temporal dynamics of CA losses and time resolved photoluminescence, we suggest that both are determined by exciton generation and recombination. © 2008 American Institute of Physics. [DOI: 10.1063/1.2840181]

In the last years, silicon nanoclusters (Si-nc) embedded in a dielectric matrix have been studied for different applications in silicon photonics. One motivation is their high efficiency as light emitters where excitation can be via optical pumping¹ as well as via current injection.² Optical gain in interface radiative states was demonstrated by several research groups,^{3–8} rising further interest in this material. Several potential applications of Si-nc for photonic devices operating in the third telecommunication window were also suggested: all-optical logical gates based on the positive nonlinear refractive index of Si-nc ($\sim 10^{-13}$ cm²/W) (Ref. 9) and all-optical or electrical light amplifiers based on Er-coupled Si-nc.¹⁰ Considering that these last devices are based on excitation of Si-nc in waveguides, it is therefore important to characterize both the linear and nonlinear optical losses at the wavelength of interest.

In this paper, we focus on a particular deleterious loss mechanism: the excited carrier absorption (CA). This process generates additional losses at signal wavelength and is particularly detrimental for devices where excitons are created within the Si-nc due to one photon or two photon absorption, such as in the amplifier or logic gate, respectively. Free carrier absorption (FCA) has been previously studied in bulk silicon¹¹ and it appears as responsible of the poor performance of many Si based photonics devices, such as IR detectors, Raman amplifiers, etc. A positive application of the FCA effect has been, however, found as a mechanism to realize fast electroabsorption modulators in silicon-on-insulator (SOI) waveguides.¹² Concerning Si-nc, only a couple of works has been dedicated to CA in slab waveguides by using prism coupling techniques.^{13,14} In this paper, we analyze and quantify CA on the propagation of a light signal at 1.54 μm in a rib waveguide.

The rib waveguides are based on an active layer (waveguide core layer) formed by Si-rich silicon oxide or SiO₂ (SRSO)/SiO₂ multilayers (ML), grown by reactive magnetron sputtering, and annealed at high temperatures. High resolution transmission electron microscopy observations allow

one to get a mean Si-nc size of 3–4 nm and a Si-nc density of $3.5 \pm 0.9 \times 10^{18}$ cm⁻³. More details on the ML growth can be found elsewhere.^{15,16} The core thickness is 1.9 μm and its refractive index is 1.57 with a negative birefringence of 1.4% at 633 nm,¹⁶ as measured by *m*-line technique.¹⁷ The rib waveguides have been fabricated through optical lithography and reactive ion etching. The rib height is 200 nm and the rib width is 10 μm .

CA loss measurements on rib waveguides have been performed by means of a pump and probe technique. A signal light coming from a tunable laser (1.3–1.6 μm) has been butt coupled to the waveguides through a single-mode polarization-preserving tapered fiber moved by a piezoelectric stage. The light exiting the end facet of the waveguide was measured with a Ge detector. A top-pumping geometry was used, where the pump light was provided by a cw Milenia laser (532 nm up to 10 W) and was focused on the waveguide surface into a strip 100 μm wide and 1 cm long by means of a cylindrical lens.

Time resolved photoluminescence (TR-PL) measurements were performed by pumping the core layer with the third harmonic of a Nd:YAG (yttrium aluminum garnet) laser (355 nm, pulse duration=6 ns, repetition rate=10 Hz) and detected with a visible streak camera (picosecond resolution) coupled to a monochromator.

In order to describe the phenomenon, a simplified scheme for the two possible mechanisms that could originate CA losses is assumed. Indeed, we are considering a four level model¹⁸ for the carrier population within the Si-nc, where CA may be generated either through a transition of an excited electron or by a transition of an excited hole.

To perform the analysis of the pump-probe data, we use the signal enhancement (SE) factor, which is the ratio of the intensity of the signal light transmitted when the waveguide is pumped (I_{p-p}) to the intensity of the signal light transmitted when the waveguide is not pumped (I_{probe}). When the waveguide is optically pumped, carriers are excited in the Si-nc and contribute to an additional loss term which is proportional to the number of excited carriers (N_{car}) and to their absorption cross section at the signal wavelength (σ_{CA}).

^{a)}Electronic mail: navarro@science.unitn.it.

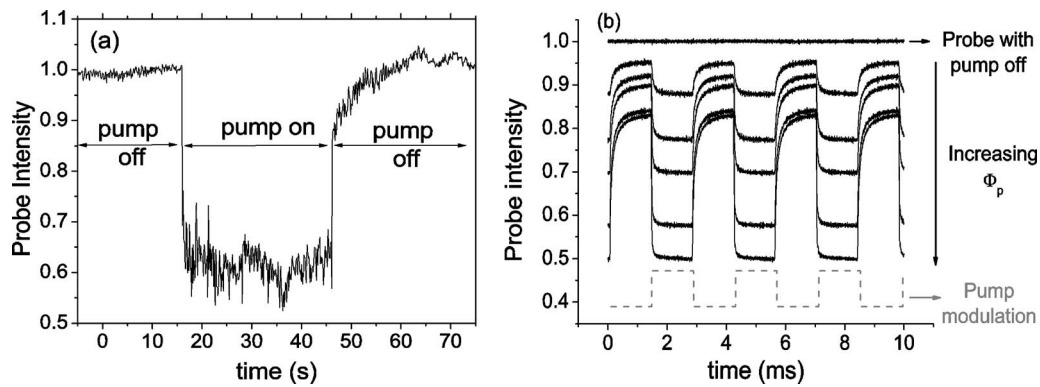


FIG. 1. Direct measurement of the intensity of a 1535 nm signal for different pump photon fluxes: (a) full temporal dynamics and (b) under chopped pump conditions (gray dashed line at the bottom).

Thus, CA loss coefficient can be written as a function of the SE in the following way:

$$\sigma_{CA} N_{\text{carr}} = - \frac{\ln(\text{SE})}{\Gamma L_{\text{pump}}}, \quad (1)$$

where Γ is the optical mode confinement factor and L_{pump} is the length of the waveguide which is actually excited by the pump. Note that the losses given by Eq. (1) are depending exclusively of the pump photon flux only in the case of low probe signals.

In Fig. 1(a), I_{probe} is shown when the pump is switched on. A rapid decrease in the probe transmission is observed. The dynamics of the decrease is characterized by two time scales, one fast (order of microseconds) and one slow (order of seconds). The slow one is due to thermal effects while the other is due to excited CA. It is worth to say that, while the fast process is extremely sensible to the alignment of the pump beam over the rib channel, the slow process is less sensitive: even if the pumped stripe is several hundreds of microns off the rib, a slow effect on the probe transmission is observed.

To separate the thermal effects from the excited CA, we chopped the pump light with a frequency faster than the dynamics of the slow process (about 0.1 Hz). Thermal effects are thus observed in probe transmission as a constant offset overimposed to the excited carrier absorption [Fig. 1(b)].

When the waveguide is pumped, the transmitted intensity decreases with a characteristic time which is a few microseconds long. The recovery of the transmitted intensity when the pump is switched off is fast but not complete: in fact, the probe signal tends to saturate at a value which is offset with respect to the no-pump probe signal. This offset is due to thermal contribution and in fact grows with Φ_p . To extract the excited carrier contribution, one has thus to consider only the decrease of the probe signal with respect to the thermal offset and not to the no-pump signal level.

Once applying Eq. (1) to the data of Fig. 1(b), the maximum of the excited CA losses as a function of the pump photon flux Φ_p is determined, as shown in Fig. 2. A square-root Φ_p dependence of $\sigma_{CA} N_{\text{carr}}$ is observed. Since σ_{CA} is independent of Φ_p , $N_{\text{carr}} \sim \Phi_p^{1/2}$. This is an indication of Auger dominated recombination processes in the Si-nc,^{18,19} possibly between close Si-nc due to their particular close distribution in the multilayered samples. Time resolved luminescence measurements performed on the very same ac-

tive core material support the presence of a strong Auger recombination mechanism at high pump photon fluxes (see inset of Fig. 2).

At the highest pump photon flux used, a maximum loss value of $1.4 \pm 0.1 \text{ cm}^{-1}$ is measured, which corresponds to $6.1 \pm 0.4 \text{ dB/cm}$. Although we do not have a direct measurement of the number of generated carriers, if Auger recombination mechanisms are strong enough, we can make the assumption that at most, one carrier per Si-nc is present at the highest photon flux. Since the Si-nc density is $3.5 \times 10^{18} \text{ cm}^{-3}$, an effective carrier absorption cross section of about $4 \times 10^{-19} \text{ cm}^2$ can be extracted. This value is one order of magnitude lower than that reported for bulk Si.²⁰

We checked this value in another rib waveguide with a core layer formed by the same Si-nc layer but a thinner SiO_2 layers. The Si-nc density for this core layer is $5.1 \pm 0.9 \times 10^{18} \text{ cm}^{-3}$ (1.5 times larger than in the previous sample). We found very similar trends in the CA losses with a maximum loss value of $2.8 \pm 0.2 \text{ cm}^{-1}$ at the highest pump photon flux. This loss value is a factor of 2 larger than that measured for the previous sample. As expected, with increasing the Si-nc density, we observed an increased excited carrier absorption which scales linearly with the Si-nc density.

The dynamics of the excited carrier absorption has been studied (Fig. 3, gray curve of bottom panel). The rise and decay line shapes can be fitted by a stretched exponential (dashed curves of bottom panel of Fig. 3) according to the following equations:

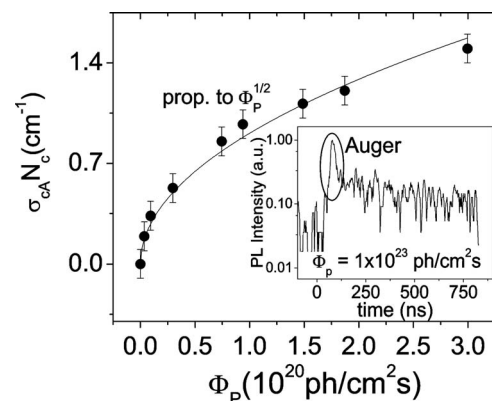


FIG. 2. Carrier absorption losses of 1535 nm signal as a function of the pump photon flux. A square-root fit to the experimental data is also shown (solid line). Inset: time resolved photoluminescence measurement performed at a pump photon flux of 1×10^{23} photons/s cm^2 .

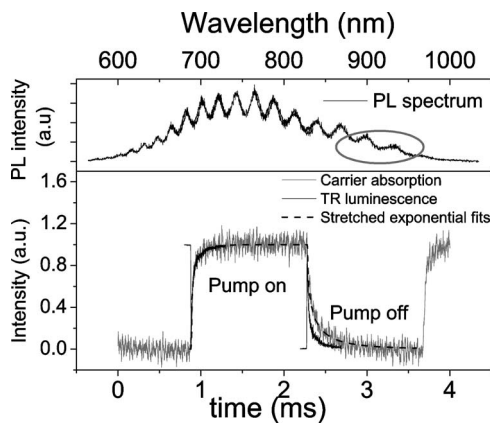


FIG. 3. Top panel: photoluminescence spectrum of the studied sample (interference fringes are observed because of large sample thickness). Bottom panel: normalized dynamical behavior of the excited carrier absorption losses (gray curve). The TR-PL decay (black right) and 1-(TR-PL) decay (black left) line shapes overlapped the CA signal. The TR-PL decay corresponds to that of the spectral range evidenced with a gray circle on the top panel, i.e., around 900 nm. Stretched exponential fits of CA are also shown (black, dashed).

$$\text{rise} \rightarrow \sigma_{CA} N_{carr}(t, \Phi) = \sigma_{CA} N_{carr}(\Phi) \left\{ 1 - \exp \left[- \left(\frac{2t}{\tau_{rise}} \right)^\beta \right] \right\},$$

$$\text{decay} \rightarrow \sigma_{CA} N_{carr}(t, \Phi) = \sigma_{CA} N_{carr}(\Phi) \exp \left[- \left(\frac{2t}{\tau_{decay}} \right)^\beta \right], \quad (2)$$

where τ_{rise} and τ_{decay} are the rise and the decay times, respectively, $N_{carr}(\Phi)$ is the number of carriers achieved in the stationary regime, and β the dispersion factor related to the curvature of the decay line shape. The results of a fit of the CA data are 20 μ s for the rise time and 60 μ s for the decay time, while the β factor is 0.5 for both cases.

A stretched exponential dynamics is also obtained when measuring the recombination of excitons in Si-nc by means of TR-PL. Many authors have tried to explain the physical origin of this kind of dynamics with different theories,²¹⁻²⁴ without reaching a consensus so far. A comparison between the time dependent excited carrier absorption and the TR-PL at about 900 nm is reported in Fig. 3. The stretched exponential best fit of the TR-PL data gives a time of 20 μ s and a β factor of 0.5, in very good agreement with the CA results for the rise time. This suggests that the excited carrier relaxation is the responsibility of the dynamics in both kinds of experiments, although they refer to very different optical transitions. An interesting result is that the agreement within the temporal dynamics is observed for the longer wavelengths only. In fact, the luminescence decay time gets shorter at shorter wavelength as characteristic of Si-nc. This indicates that CA is mainly due to large Si-nc. The decay time observed in the CA data is slightly longer than that measured by TR-PL. This could be also associated to a modification of the excited state due to the absorption of the signal light, thus, delaying the relaxation mechanisms toward the fundamental state. Indeed, we have observed that for the same pump photon flux conditions, the carrier absorption losses get reduced when the probe signal intensity is increased. This means that the exciton population is indeed affected by the probe light intensity and in this specific regime, Eq. (1) depends also on the probe signal intensity.

In conclusion, excited carrier absorption in Si-nc has been characterized and quantified in rib-waveguides by mea-

suring the pump power dependent propagation losses at 1535 nm. These results are relevant for photonic system based on heavily optically pumped Si-nc waveguides.

As a consequence of the presence of the pumping light, two independent loss mechanisms appear that behave with very different temporal dynamics: one is slow (seconds) that is related with thermal effects and affects the waveguiding properties and a second is fast (microseconds) that is associated to the excited carrier absorption. The excited carrier absorption has the same characteristic dynamics of the recombination of exciton luminescence in large Si-nc. This indicates that the way to reduce the excited carrier absorption is to decrease the Si-nc size in the waveguide.

The authors would like to thank the financial support by EC through the projects PHOLOGIC (FP6-017158) and LANCER (FP6-033574).

- ¹S. Ossicini, L. Pavesi, and F. Priolo, *Light Emitting Silicon for Microphotonics*, Selected Topics in Modern Physics Vol. 194 (Springer, Berlin, 2003).
- ²Z. Gaburro and L. Pavesi, in *Handbook of Luminescence, Display Materials and Devices*, edited by H. S. Nalwa and L. Shea Rohwer (American Scientific, Stevenson Ranch, USA, 2003), Vol. 3, p. 101.
- ³L. Pavesi, L. Dal Negro, C. Mazzoleni, G. Franzò, and F. Priolo, *Nature* (London) **440**, 408 (2000).
- ⁴L. Pavesi, *J. Phys.: Condens. Matter* **R1169**, 15 (2003).
- ⁵L. Dal Negro, M. Cazzanelli, L. Pavesi, S. Ossicini, D. Pacifici, G. Franzò, F. Priolo, and F. Iacona, *Appl. Phys. Lett.* **82**, 4636 (2003).
- ⁶L. Khriachtchev, M. Rasanen, S. Novikov, and J. Sinkkonen, *Appl. Phys. Lett.* **79**, 1249 (2001).
- ⁷M. Nayfeh, S. Rao, N. Barry, A. Smith, and S. Chaieb, *Appl. Phys. Lett.* **80**, 121 (2002).
- ⁸K. Luterova, I. Pelant, I. Mikulskas, R. Tomasiunas, D. Muller, J. J. Grob, J. L. Rehspringer, and B. Hönerlage, *J. Appl. Phys.* **91**, 2896 (2002).
- ⁹R. Spano, M. Cazzanelli, N. Daldosso, Z. Gaburro, L. Ferraioli, L. Tartara, J. Yu, V. Degiorgio, S. Hernandez, Y. Lebour, P. Pellegrino, B. Garrido, E. Jordana, J. M. Fedeli, and L. Pavesi, *Group IV Semiconductor Nanostructures-2006*, MRS Symposia Proceedings No. 958 (Materials Research Society, Pittsburgh, 2007) p. L08-06.
- ¹⁰N. Daldosso, D. Navarro-Urrios, M. Melchiorri, C. Garcia, P. Pellegrino, B. Garrido, C. Sada, G. Battaglin, F. Gourbilleau, R. Rizk, and L. Pavesi, *IEEE J. Sel. Top. Quantum Electron.* **12**, 1607 (2006).
- ¹¹W. Spitzer and H. Y. Fan, *Phys. Rev.* **108**, 268 (1957).
- ¹²M. Lipson, *IEEE J. Sel. Top. Quantum Electron.* **12**, 1520 (2006).
- ¹³M. Forcales, N. J. Smith, and R. G. Elliman, *J. Appl. Phys.* **100**, 014902 (2006).
- ¹⁴N. Smith, M. J. Lederer, M. Samoc, M. J. Luther-Davies, and R. G. Elliman, *Optoelectronics of Group-IV-Based Materials*, MRS Symposia Proceedings No. 770 (Materials Research Society, Pittsburgh, 2003), pp. I3.2.1-6.
- ¹⁵C. Ternon, F. Gourbilleau, X. Portier, P. Voivenel, and R. Rizk, *Thin Solid Films* **419**, 5 (2002).
- ¹⁶N. Daldosso, M. Melchiorri, L. Pavesi, G. Pucker, F. Gourbilleau, S. Chausserie, A. Belarouci, X. Portier, and C. Dufour, *J. Lumin.* **121**, 2 (2006).
- ¹⁷P. K. Tien, *Appl. Opt.* **10**, 2395 (1971).
- ¹⁸L. Dal Negro, M. Cazanelli, N. Daldosso, Z. Gaburro, L. Pavesi, F. Priolo, D. Pacifici, G. Franzò, and F. Iacona, *Physica E (Amsterdam)* **16**, 297 (2003).
- ¹⁹R. M'ghaieth, H. Maâref, I. Mihalcescu, and J. C. Vial, *Phys. Rev. B* **60**, 4450 (1999).
- ²⁰A. Green, *Silicon Solar Cells* (University of New South Wales, Sydney, 1995), p. 48.
- ²¹L. Pavesi and M. Ceschini, *Phys. Rev. B* **48**, 17625 (1993).
- ²²J. Ventura, M. C. do Carmo, and K. P. O'Donnell, *J. Appl. Phys.* **77**, 323 (1995).
- ²³J. Linnros, N. Lalic, A. Galeckas, and V. Grivickas, *J. Appl. Phys.* **86**, 6128 (1999).
- ²⁴C. Delerue, G. Allan, C. Reynaud, O. Guillois, G. Ledoux, and F. Huisken, *Phys. Rev. B* **73**, 235318 (2006).